Cellular and Molecular Biology
E-ISSN : 1165-158X / P-ISSN : 0145-5680
www.cellmolbiol.org

Original Research

Three-dimensional bio-printed constructs consisting of human umbilical-derived mesenchymal stem cells promote cell viability, proliferation, and differentiation *in vitro*

Qingxia Tao[1, 2#], Cuiying Wu[1#], Xinda Li[3], Wenjin Chen[4], Kai Sun[5], Peng Zhang[1], Zhijun Yang[1], Ning Liu[1], Ruxiang Xu[6, 1*], Tao Xu[3*], Chong Wang[8*]

[1] Department of Neurosurgery, Affiliated Bayi Brain Hospital, the Seventh Medical Center of PLA General Hospital, Beijing, 100700, People's Republic of China
[2] Department of Surgery, NO.1 LanShan People's hospital, lin-yi City, Shandong Province, 276002, People's Republic of China
[3] Biomanufacturing and Rapid Forming Technology Key Laboratory of Beijing, Department of Mechanical Engineering, Tsinghua University, Beijing 100084, People's Republic of China
[4] Department of Neurosurgery, Affiliated Bayi Brain Hospital, the Seventh Medical Center of PLA General Hospital, Southern Medical University, Guangzhou, 100000, People's Republic of China
[5] Department of Neurosurgery, Affiliated Bayi Brain Hospital, the Seventh Medical Center of PLA General Hospital, Army Medical University, Chongqing, 400038, People's Republic of China
[6] Department of Neurosurgery, Sichuan Academy of Medical Sciences and Sichuan Provincial People's Hospital, School of Medicine, University of Electronic Science and Technology of China, Chengdu 610072, Sichuan, China
[7] Department of Precision Medicine and Healthcare, Tsinghua-Berkeley Shenzhen Institute, Shenzhen 518055, People's Republic of China
[8] Affliated Zhoupu Hospital, Shanghai University of Medicine and Health Sciences, Shanghai 310115, People's Republic of China

[*]**Correspondence to:** jhwq26@163.com

Received November 25, 2019; **Accepted** May 8, 2020; **Published** May 15, 2020

[#]These authors contributed equally to this work.

Doi: http://dx.doi.org/10.14715/cmb/2020.66.2.27

Abstract: The aim of this study was to investigate the effect of three-dimensional (3D) bio-printed constructs consisting of human umbilical-derived mesenchymal stem cells (HUMSCs) on cell viability, proliferation and differentiation *in vitro*. Functional 3D bio-printed microspheres consisting of HUMSCs were constructed using electrostatic inkjet technique. The parameters used for the synthesis of 3D bio-printed tissue constructs were first optimized. The viability, proliferation and differentiation of 3D cultured HUMSCs were assessed. The results of scanning electron microscopy (SEM) showed that isolated HUMSCs exhibited fibroblast-like spindle adherent growth. The optimized printing parameters were 6 kV voltage, 10 mL/h flow, 15 cm receiving height, and alginate: water ratio of 1:1 mixed at 37 °C. Compared with 2D cultured HUMSCs, the 3D cultured HUMSCs have better viability, proliferation and differentiation ability. The results obtained in this study indicate that 3D bio-printed tissue constructs promote HUMSC viability, proliferation, and neural differentiation *in vitro*.

Key words: Human umbilical-derived mesenchymal stem cell; Three-dimensional bioprinted microspheres; Viability; Proliferation; Bio-electrospraying.

Introduction

Three-dimensional (3D) printing technology has attracted huge attention in the field of Biomedical Science, and has so far yielded many positive results (1, 2). Studies have shown that cells in 3D structures are capable of mimicking the microenvironment *in vivo,* and exhibit improved engraftment property (3, 4). Bio-electrospraying (BES) technology is an important technique for direct and efficient delivery of cells in the form of a jet. Although methods such as ink-jet printing (IJP) and aerodynamically-assisted bio-jets (AABJ/T) are used for direct cell handling, they have been shown to reduce cell viability. The association of BES with scaffold production techniques has been shown to be an interesting strategy for the production of biomaterials with cells homogeneously distributed in the entire structure. Several studies have evaluated the effects of BES on different cell types. However, little or nothing is known about its impact on mesenchymal stem cells (MSCs). The BES technique has less impact on cell viability (5). Human umbilical-derived mesenchymal stem cells (HUMSCs) constitute an attractive source of stem cells for clinical therapies because they are easily obtained, multipotent, free of ethical or legal conflicts, and show little immunologic rejection (6, 7). However, their slowness to differentiation and low levels of cell aggregation in lesion sites are two important factors that have limited their clinical application. The development of new methods that can sufficiently overcome these limitations has become necessary. In this study, BES technique was used to engineer a functional 3D scaffold for encapsulation of HUMSCs, and the impact of BES technique on their viability, proliferation and differentiation *in vitro* was investigated.

Materials and Methods

Materials

Glial fibrillary acidic protein (GFAP), rabbit anti-CD105, anti-beta III tubulin, anti-nestin, anti-MAP2, and anti- GAPDH antibodies were obtained from Abcam (USA). Galactosylceramidase (GALC) antibody was purchased from Proteintech (USA); CellTracker CM-DiI dye was a product of Yesen (Thialand), while recombinant human brain-derived neurotrophic factor (BDNF), basic fibroblast growth factor (bFGF) and epidermal growth factor (EGF) were purchased from Peprotech (USA). Dulbecco's modified Eagle medium/ Ham's F-12 medium (DMEM-F12) was obtained from Hyclone (USA). Fetal bovine serum (FBS), 0.25 % trypsin-EDTA, and B-27 serum-free supplement (50X) were products of Gibco (USA). Fluorescent live/dead viability assay kit, radioimmunoprecipitation lysis (RIPA) buffer, and bicinchoninic acid (BCA) protein assay kit were obtained from KeyGEN Biotech (China). Alamar Blue cell viability kit was purchased from Yeasen Biotechnology Ltd. (China). Alexa 488-conjugated goat anti-mouse immunoglobulin G was purchased from Beyotime (China). Mounting medium containing 4, 6-diamidino-2-phenylindole (DAPI) was obtained from Vectashield Vector Laboratories (USA). Goat anti-rabbit IgG/HRP was produced by Southern Biotech (USA). Rabbit anti-goat IgG/HRP was a product of Golden Bridge International (USA). Human MSC analysis kit was purchased from BD Biosciences (USA); Moflo XDP flow cytometer was obtained from Beckman Coulter Inc. (USA), while microplate reader was purchased from BioTek (USA). Carbon dioxide critical point dryer was a product of LEICA (USA), while ULTRA 55 scanning electron microscope was a product of ZEISS (Germany). Image J software was obtained from Rawak Software Inc. (Germany).

Isolation of HUMSCs and culture

Human MSCs were isolated from umbilical cords of healthy pregnant women after obtaining written informed consents from them. The procedures used in this study were approved by the Ethics Committee of the Seventh Medical Centre of Chinese PLA General Hospital, China. Isolated HUMSCs were cultured as described in literature, with slight modification (6, 10). Immediately after the arteries and veins of fresh human umbilical cords were removed, the remaining Wharton's jelly tissue was cut into bits (0.5 – 1 cm^3), seeded in 10-cm^2 petri dish, and cultured in DMEM-F12 supplemented with 10 % FBS and 1 % penicillin/streptomycin solution at 37 ˚C for 24 h in a humidified atmosphere of 5 % CO_2 and 95 % air. The medium was refreshed every two days. After 1 week of incubation, the adherent confluent cells were trypsinized with 0.25 % trypsin-EDTA, and then cultured again and passaged for later use. Cells in logarithmic growth phase were selected and used for this study.

Immunophenotypic analysis of HUMSCs

Immunophenotypic analysis of HUMSCs was carried out using a flow cytometer. After passage 3, the cells were collected and prepared into a single-cell suspension, and then subjected to immunophenotypic analysis using a Moflo XDP flow cytometer fitted with analysis software. The analysis was performed using human MSC analysis kit. At least 10,000 events were acquired per time. The percentage of cells positive for each antigen was evaluated from at least three independent experiments.

Induction of neural differentiation of HUMSCs

The HUMSCs were seeded in 24-well plates at a density of 1 x 10^7 cells/well and cultured in DMEM-F12 supplemented with 10 % FBS. Neural differentiation of the cells was induced by culturing them in neurobasal medium supplemented with 2 % B27, 10 ng/mL EGF, and 20 ng/mL bFGF according to literature (8-10). The medium was changed every 4 days. The morphology of the cells was observed under an optical microscope.

Controlled release studies

Injectable microspheres were obtained using BES technology. Sodium alginate was sterilized using gamma radiation, and dissolved in sterile deionized water at concentrations of 4, 2, 1, and 0.5 % (w/v). Sodium alginate and culture medium were mixed at a ratio of 1:1 at 37 °C for use in spraying. The spraying voltage was set at 10 kV. The gel flow was 10 mL/h and the spraying height was 15 cm. Exactly 1 % sodium alginate solution was used and the voltage was in the range of 0 – 12 kV. The flow was varied (1 – 10 mL/h), and the receiving heights were set at 5, 10, 15, and 20 cm. After spraying, the microspheres were immersed in 3% calcium chloride solution for cross-linking, and then washed with sterile deionized water. The cell microspheres were collected and imaged using a light microscope to measure their diameter.

Cell viability assay

The viability of HUMSCs in 3D cultures was assessed using fluorescent live/dead viability assay kit at 3 h and 7 days immediately after BES. After 15 min of incubation at 37 °C, propidium iodide (PI) and calcein-AM were removed by washing thrice with phosphate-buffered saline (PBS), and the samples were observed under a fluorescence microscope. For each sample (n = 3), at least ten different random fields were examined. A total of 1000 cells were counted to obtain living (green) cells. In addition, dead cells (red) were PI positive.

Cell proliferation assay

Human umbilical-derived mesenchymal stem cell (HUMSC) proliferation was assessed using **Alomar** Blue kit on days 1, 4, 7, 10, 13, and 16 after BES. A control group with the same initial cell number was cultured in two-dimension (2D). The Alomar Blue working solution (5 mL/dish) was added to the cells and subsequently incubated at 37 °C for 2 h. The supernatant of each sample was transferred to 96-well culture plates and the absorbance read at 570 nm using an automated microplate reader. The procedure was performed in triplicate.

Scanning electron microscopy (SEM)

Human umbilical-derived mesenchymal stem cell (HUMSC) microspheres were fixed in 2.5 % glutaraldehyde overnight at 4 °C. This was followed by addi-

tion of 30 % ethanol and incubation at room temperature for 15 min. The samples were subsequently dehydrated for 30 min using a gradient of ethanol concentrations (50, 70, 90 and 100 %), and dried using carbon dioxide critical point dryer. The resultant microspheres were coated with platinum and imaged using an ULTRA 55 scanning electron microscope.

Immunofluorescence analysis

In order to enhance cell dissociation, the microspheres were immersed in dissociation solution containing 0.9 % NaCl, 55 mM sodium citrate, and 20 mM ethylenediaminetetraacetate (EDTA) for 5 min. The cells were thereafter collected and re-seeded in 6-well plates at 37 °C for 12 h to allow them adhere properly to the plates. The 2D-cultured cells were also treated in a ssimilar manner. The two groups were fixed in 4 % paraformaldehyde at room temperature for 30 min and permeabilized with 0.1 % Triton X-100 for 20 min. They were then incubated overnight with primary antibodies (CD105, MAP2, GFAP, and GALC), followed by incubation with secondary antibodies.

Western blotting

The cells were washed twice with PBS and lysed with 100 µL of ice-cold RIPA buffer containing protease and phosphatase inhibitors. The resultant lysate was centrifuged at 10,000 rpm for 20 min at 4 °C, and the protein concentration of the supernatant was determined using BCA method. A portion of total cell protein (30 µg) from each sample was separated on 8 % SDS-polyacrylamide gel electrophoresis and transferred to a fixed polyvinylidene fluoride membrane at 110 V and 90 °C for 120 min. Subsequently, non-fat milk powder (5 %) in Tris-buffered saline containing 0.2 % Tween-20 (TBS-T) was added with gentle shaking at 37 °C and incubated to block non-specific binding of the blot. The blots were incubated overnight at 4 °C with the primary antibodies rabbit polyclonal anti-CD105, MAP2, GFAP, GALC and GAPDH, each at a dilution of 1 to 800. Thereafter, the membrane was washed thrice with PBS and further incubated with horseradish peroxidase-conjugated goat anti-rabbit IgG secondary antibody for 1.5 h at room temperature. The blot was developed using an X-ray film. Grayscale analysis of the bands was performed using ECL. The respective protein expression levels were normalized to that of GAPDH which was used as a standard.

Statistical Analysis

Data are expressed as mean ± SEM. Statistical analysis was performed using SPSS (19.0). Groups were compared using Student's *t*-test. Statistical significance was assumed at $p < 0.05$.

Results

Characterization of HUMSCs

The results of SEM showed that isolated HUMSCs exhibited fibroblast-like spindle adherent growth (Figure1 A). The HUMSCs were CD105 (99.52 %), CD90 (97.62 %), CD73 (96.88 %), and CD44 (99.95 %) positive, but CD45, CD34, CD11b, CD19, and HLA-DR negative (Figures 1 B – 1F).

Optimization of parameters for synthesis of 3D bio-printed tissue constructs

Human umbilical-derived mesenchymal stem cell (HUMSC)-laden alginate microspheres were successfully produced using BES (Figure 2). In order to obtain suitable 3D bio-printed tissue constructs, alginate concentration, spraying voltage, and hydrogel flow were optimized. It was found that the diameter of the microspheres was dependent on hydrogel concentration. Alginate concentration was directly proportional to microsphere diameter (the higher the concentration of alginate, the larger the diameter of microspheres) (Figure 2A). There was a decrease in microsphere size when the spraying voltage was increased from 0 to 6 kV. However, when the voltage exceeded 6 kV, the microspheres became unstable and cell viability decreased significantly ($p < 0.05$). After repeated verifications, the optimal voltage was found to be 6 kV (Figure 2B). There was a direct relationship between hydrogel flow and microsphere diameter: as the hydrogel flow increased, the diameter of cell microspheres also increased (Figure 2C). The optimal hydrogel flow was 10 mL/h. There was no clear relationship between particle size and receiving height (Figure 2D). Based on the height of available operating table, a 15-cm receiving height was

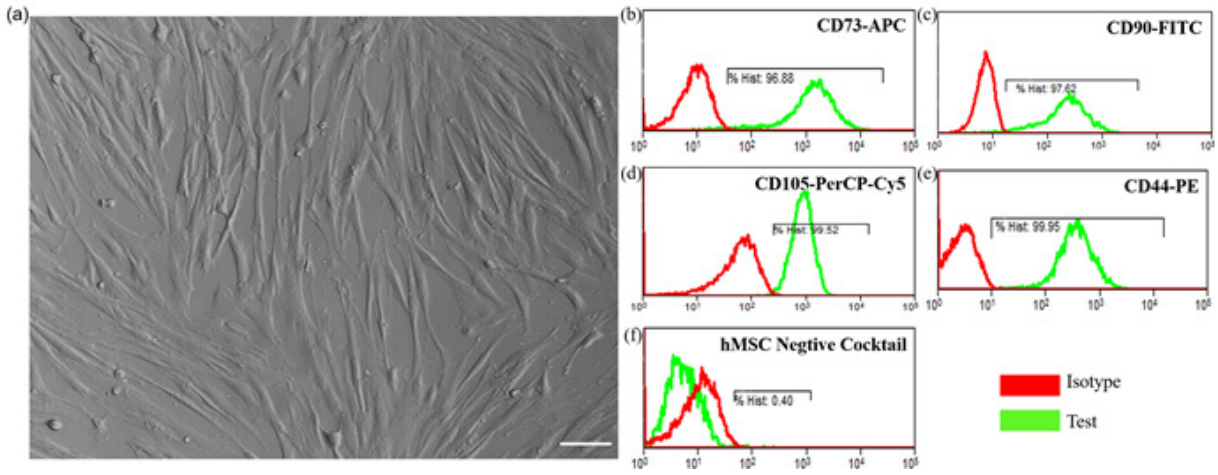

Figure 1. Morphological and immunophenotypic analysis of isolated HUMSCs. (A): Passage 3 HUMSCs displayed a fibrocyte-like form with long fusiform shape (scale bars = 30 µm). (B – F): Flow cytometric analysis of passage 3 HUMSCs using human MSC analysis kit.

selected. After optimization of the printing parameters, 3D bio-printed constructs consisting of HUMSCs with regular shape were obtained (Figures 2E and 2F).

Viability of 3D bio-printed tissue constructs in vitro

Live cells produced green fluorescence, while dead cells produced red fluorescence after staining (Figure 3). Highly viable cells were evenly distributed in the hydrogel scaffolds. Cell viability on day 7 was significantly higher than that at 3 h after printing ($p < 0.05$; Figures 3A – 3F).

Proliferation of 3D bio-printed tissue constructs in vitro

The proliferation of 2D cells was significantly higher than that of 3D cells in the early stage, and peaked on day 7 ($p < 0.05$). However, 3D cell proliferation was significantly higher than that of 2D cell in the later phases ($p < 0.05$; Figure 4A). Images from SEM showed that sodium alginate enwrapped and supported cells growing in the spheroids, and cells close to the edge of the microspheres exhibited tendency to migrate from the core (Figures 4B and 4C).

Expressions of GFAP, GALC, and MAP2 in 3D environment

Constructs cultured in 3D induction environment significantly upregulated the expressions of GFAP, GALC, and MAP2, but significantly down-regulated CD105 protein expression, when compared with their corresponding expressions in 2D environment ($p < 0.05$; Figures 5A and 5B). Immunofluorescence staining for

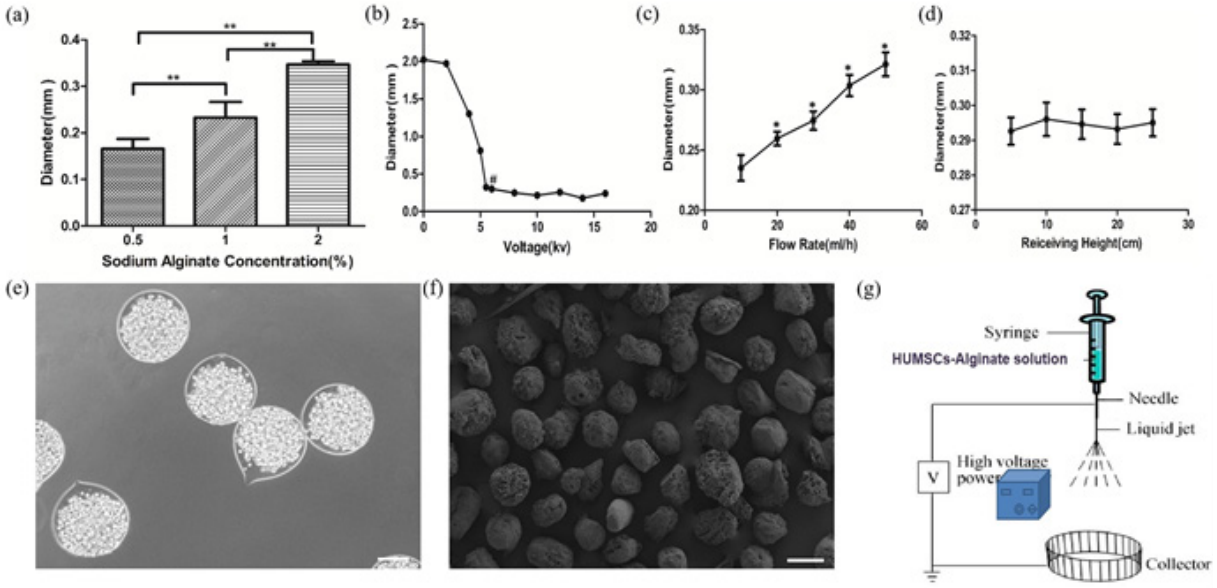

Figure 2. Optimization of parameters for the synthesis of 3D bio-printed tissue constructs. (A – D): Mixture printed with different alginate concentrations, voltages, flows, and receiving heights. (A): Optimal concentration of alginate was 1 %. (B): Optimal voltage was 6 kV (C): Optimal hydrogel flow was 10 mL/h (D): The size of the microspheres had no obvious relationship with the receiving height (E): Formation of consistent stable cell microspheres as shown using a light microscope (D): Formation of consistent stable cell microspheres as shown using an electron microscope (F):. Schematic representation of cell microsphere printing (scale bar = 100 μm) (G): Schematic representation of the entire procedure. $^{*}p < 0.05$, $^{**}p < 0.01$, compared with cells in 2D print; $^{\#}$optimal voltage based on the experience.

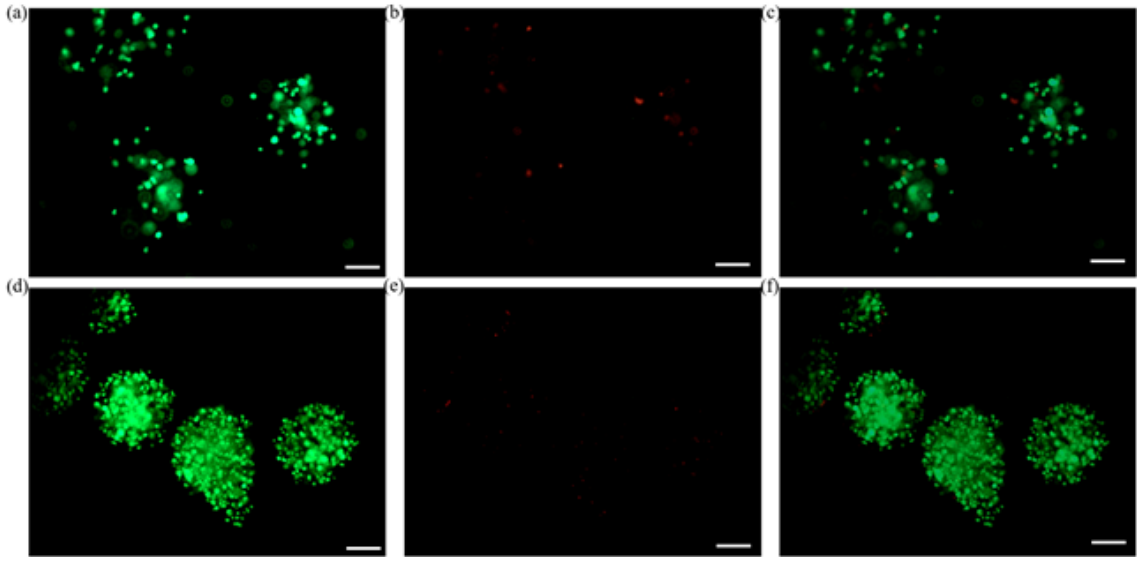

Figure 3. Cell viability of 3D bio-printed tissue constructs. (A – C): Live/dead staining of cells 2 h after BES, with live cells stained green and dead cells stained red (scale bar = 100 μm). (D – F): Live/dead staining of cells 15 days after BES (scale bar = 100 μm).

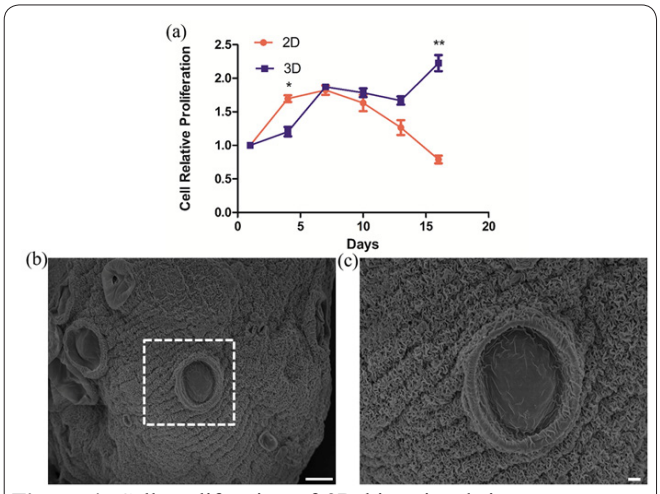

Figure 4. Cell proliferation of 3D bio-printed tissue constructs. (A): Cell proliferation of 2D and 3D constructs normalized to the OD value at day 1. (B): Ultramarine structure of cell microspheres (scale bar = 10 μm). (C): Cell migration from the core (scale bar = 2 μm). $^{*}p < 0.05$ and $^{**}p < 0.01$, when compared with control cells.

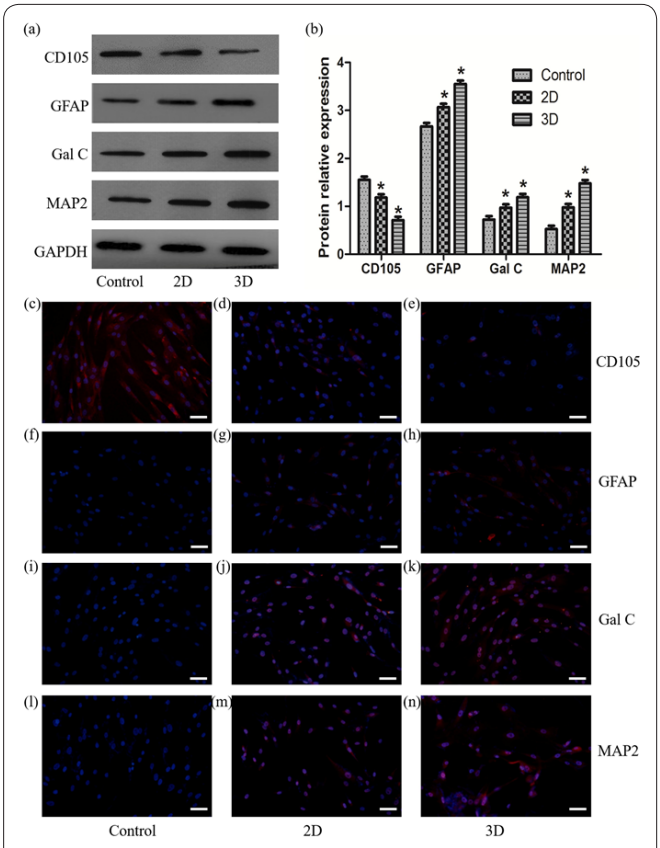

Figure 5. Cell differentiation of 3D bio-printed tissue constructs. (A): Protein expressions of CD105, GFAP, GALC, and MAP2 after induction for 3 weeks; (B): Levels of expression of CD105, GFAP, GALC, and MAP2 genes after induction for 3 weeks; (C): Expression of CD105 in control cells; (D): Expression of CD105 in 2D induction environment; (E): Expression of CD105 in 3D induction environment (scale bar = 50 μm); (F): Expression of GFAP in control cells: (G): Expression of GFAP in 2D induction environment; (H): Expression of GFAP in 3D induction environment (scale bar = 50 μm); (I): Expression of GALC in control cells; (J): Expression of GALC in 2D induction environment; (K): Expression of GALC in 3D induction environment (scale bars = 50 μm); (L): Expression of MAP2 in control cells; (M): Expression of MAP2 in 2D induction environment; (N): Expression of MAP2 in 3D induction environment (scale bar = 50 μm). $^{*}p < 0.05$, when compared with control cells.

CD105 showed that constructs cultured in 3D induction environment significantly down-regulated CD105 protein expression after 3 weeks relative to its corresponding expression in 2D induction environment ($p < 0.05$; Figures 5C – 5E). The results of immunofluorescence staining for GFAP, GALC, and MAP2 in 3D induction environment on day 14 indicate that their expressions were significantly upregulated, when compared with values for 2D induction environment (Figures 5F – 5N).

Discussion

Human umbilical-derived mesenchymal stem cells (HUMSCs) are used in transplantation for traumatic brain injury (TBI). However, their effectiveness is limited due to poor differentiation and cell loss after transplantation. Effective cell induction and delivery modality are technological challenges for successful clinical application of HUMSC-based therapies. In this study, a novel microencapsulation technique was designed to produce alginate-HUMSC microspheres. The results indicate that induction of HUMSCs to differentiate within the microspheres stimulated the cells to rapidly differentiate to neural lineage specific cells. These results are in agreement with those of previous reports (11, 12).

Three-dimensional (3D) microenvironment is closer to the physiological growth conditions of cells where the connection between cells or cells and the extracellular matrix (ECM) is greatly increased (13, 14). The size of a microsphere can be controlled and optimized by adjusting the BES parameters. In this study, cell proliferation and differentiation were preserved/strengthened in the hydrogel structure of printed cells, when compared with 2D culture conditions. These results are in agreement with those reported previously (15). It is likely that BES-constructed microspheres promote the proliferation and differentiation of HUMSCs.

Bio-electrospraying (BES) is a new technology that enables the deposition of living cells on various targets with a resolution that depends on cell size and rather than the jetting phenomenon. It is widely used in pharmaceutical research, fabrication of biological scaffolds, and delivery of bioactive proteins. It is highly efficient and convenient. However, controlling the size of microspheres while maintaining high cell viability after BES are fundamental to achieving successful injectable 3D cell models and maintenance of cell functions (16). Alginate is a common term used for a family of unbranched polymers that form ionic bonds with divalent cations (usually Ca^{2+}) to give a 3D network structure. Sodium alginate possesses good biocompatibility and desirable mechanical properties after crosslinking (17, 18). The stable stereo-chemical structure and diameter of the cell-gel formed are dependent on the concentration of alginate.

In this study, when the concentration of sodium alginate was higher than 2 %, coupled with increased viscosity, the size of the microspheres formed increased. However, the production of adjoint droplet and fragile gel made cell microspheres irregular (19). When sodium alginate concentration was lower than 0.5 %, the shape of the cell microsphere produced was irregular, and it readily fragmented when the culture medium

was changed. In addition, strong mechanical constraints significantly inhibited cell growth. Comprehensive consideration led to the use of 1 % alginate which not only provided strong structural support for the bio-printed microspheres, but also provided an appropriate microenvironment for maintenance of cell viability, appropriate diameter, and permeability (20). Alginate decomposes gradually and completely disappears after 8 weeks, which is an important characteristic for the printed structures (21-24). Voltage is a key factor that determines the diameters of microspheres and cell viability. The results of this study indicate that 6 kV was the optimum voltage that resulted in minimal cell injury.

The primary injury observed in HUMSCs encapsulated in microspheres might have been due to cell-alginate mixing, voltage, and crosslinking of calcium ions. In this study, dead cells were gradually degraded with time, while live cells proliferated. The proliferation of HUMSCs encapsulated in printed constructs was significantly increased throughout the observation period. In the initial phase (days 1 – 7), the proliferation of 2D cultured cells was significantly increased, relative to that of 3D cells. It is possible that there was a temporary attrition of HUMSCs after BES in 3D collagen-based matrices. These results are similar to those observed for ink-jet and extrusion-based printings (25-27). However, in the later phase (days 7 – 16), the proliferation of 2D cultured cells was significantly reduced, indicating contact inhibition. These results suggest that BES structures may have provided enough space for maintenance of a certain number of cells and support long-term cell proliferation.

The results obtained in this study indicate that 3D bio-printed tissue constructs promote HUMSC viability, proliferation, and neural differentiation *in vitro.*

Acknowledgments
This study was funded by the Military Medical Science Research Project (No. 16CXZ001) and the National Natural Science Foundation of China (No. 81601085). The authors would like to thank all the anonymous reviewers for their valuable comments on how to improve the quality of this paper. We thank Sarah Dodds, PhD, from Liwen Bianji, Edanz Editing China (www.liwenbianji.cn/ac), for editing the English text of a draft of this manuscript.

Conflict of Interest
There are no conflicts of interest in this study.

Contributions of authors
All work was done by the author named in this article and the authors accept all liability resulting from claims which relate to this article and its contents. The study was conceived and designed by Ruxiang Xu, Tao Xu and Chong Wang; Qingxia Tao, Cuiying Wu, Xinda Li, Wenjin Chen, Kai Sun, Peng Zhang, Zhijun Yang, Ning Liu, Ruxiang Xu, Tao Xu, Chong Wang collected and analysed the data; Qingxia Tao and Cuiying Wu wrote the text and all authors have read and approved the text prior to publication.
Qingxia Tao and Cuiying Wu contributed equally to this work and should be considered as co-first authors.
Ruxiang Xu, Tao Xu and Chong Wang are co-corresponding authors.

References

1. Ji S, Guvendiren M. Recent Advances in Bioink Design for 3D Bioprinting of Tissues and Organs. Front Bioeng Biotechnol 2017; 5: 23.
2. Murphy SV, Atala A. 3D bioprinting of tissues and organs. Nat Biotechnol 2014; 32: 773-785.
3. Kong M, Hong SE. Comparison of survival rates between 3D conformal radiotherapy and intensity-modulated radiotherapy in patients with stage III non-small cell lung cancer. Onco Targets Ther 2016; 9: 7227-7234.
4. Oltolina F, Zamperone A, Colangelo D, Gregoletto L, Reano S, Pietronave S. Human Cardiac Progenitor Spheroids Exhibit Enhanced Engraftment Potential. Plos One 2015; 10: 137999.
5. Saunders RE, Gough JE, Derby B. Delivery of human fibroblast cells by piezoelectric drop-on-demand inkjet printing. Biomaterials 2008; 29: 193-203.
6. Ezquer F, Ezquer M, Arango-Rodriguez M, Conget P. Could donor multipotent mesenchymal stromal cells prevent or delay the onset of diabetic retinopathy? Acta Ophthalmol 2014; 92: 86-95.
7. Nagamura-Inoue T, He H. Umbilical cord-derived mesenchymal stem cells: Their advantages and potential clinical utility. World J Stem Cells 2014; 6: 195-202.
8. Kim ES, Ahn SY, Im GH, Sung DK, Park YR, Choi SH, et al. Human umbilical cord blood-derived mesenchymal stem cell transplantation attenuates severe brain injury by permanent middle cerebral artery occlusion in newborn rats. Pediatr Res 2012; 72: 277-284.
9. Cheng Q, Zhang Z, Zhang S, Yang H, Zhang X, Pan J, et al. Human umbilical cord mesenchymal stem cells protect against ischemic brain injury in mouse by regulating peripheral immunoinflammation. Brain Res 2015; 1594: 293-304.
10. Markiewicz I, Sypecka J, Domanska-Janik K, Wyszomirski T, Lukomska B. Cellular environment directs differentiation of human umbilical cord blood-derived neural stem cells in vitro. J Histochem Cytochem 2011; 59: 289-301.
11. Kawaguchi N, Machida M, Hatta K, Nakanishi T, Takagaki Y. Cell shape and cardiosphere differentiation: a revelation by proteomic profiling. Biochem Res Int 2013; 2013: 730874.
12. Mineda K, Feng J, Ishimine H, Takada H, Doi K, Kuno S, et al. Therapeutic Potential of Human Adipose-Derived Stem/Stromal Cell Microspheroids Prepared by Three-Dimensional Culture in Non-Cross-Linked Hyaluronic Acid Gel. Stem Cells Transl Med 2015; 4: 1511-1522.
13. Kogan EA, Namiot VA, Demura TA, Faizullina NM, Sukhikh GT. Reparative and neoplastic spheroid cellular structures and their mathematical model. Biofizika 2014; 59: 533-540.
14. Ou CW, Su CH, Jeng US, Hsu SH. Characterization of biodegradable polyurethane nanoparticles and thermally induced self-assembly in water dispersion. ACS Appl Mater Interfaces 2014; 6: 5685-5694.
15. Saha K, Keung AJ, Irwin EF, Li Y, Little L, Schaffer DV, et al. Substrate modulus directs neural stem cell behavior. Biophys J 2008; 95: 4426-4438.
16. Abeyewickreme A, Kwok A, McEwan JR, Jayasinghe SN. Bioelectrospraying embryonic stem cells: interrogating cellular viability and pluripotency. Integr Biol (Camb) 2009; 1: 260-266.
17. Rowley JA, Madlambayan G, Mooney DJ. Alginate hydrogels as synthetic extracellular matrix materials. Biomaterials 1999; 20: 45-53.
18. Sarker B, Rompf J, Silva R, Lang N, Detsch R, Kaschta J, et al. Alginate-based hydrogels with improved adhesive properties for cell encapsulation. Int J Biol Macromol 2015; 78: 72-78.

19. Ye C, He Z, Lin Y, Zhang Y, Tang J, Sun B, et al. Bio-electrospraying is a safe technology for delivering human adipose-derived stem cells. Biotechnol Lett 2015; 37: 449-456.
20. Hong J, DeMello AJ, Jayasinghe SN. Bio-electrospraying and droplet-based microfluidics: control of cell numbers within living residues. Biomed Mater 2010; 5: 21001.
21. Kim WS, Mooney DJ, Arany PR, Lee K, Huebsch N, Kim J. Adipose tissue engineering using injectable, oxidized alginate hydrogels. Tissue Eng Part A 2012; 18: 737-743.
22. Boontheekul T, Kong HJ, Mooney DJ. Controlling alginate gel degradation utilizing partial oxidation and bimodal molecular weight distribution. Biomaterials 2005; 26: 2455-2465.
23. Bouhadir KH, Lee KY, Alsberg E, Damm KL, Anderson KW, Mooney DJ. Degradation of partially oxidized alginate and its potential application for tissue engineering. Biotechnol Prog 2001; 17: 945-950.
24. Park H, Lee KY. Cartilage regeneration using biodegradable oxidized alginate/hyaluronate hydrogels. J Biomed Mater Res A 2014; 102: 4519-4525.
25. Dai X, Liu L, Ouyang J, Li X, Zhang X, Lan Q, et al. Coaxial 3D bioprinting of self-assembled multicellular heterogeneous tumor fibers. Sci Rep 2017; 7: 1457.
26. Billiet T, Gevaert E, De Schryver T, Cornelissen M, Dubruel P. The 3D printing of gelatin methacrylamide cell-laden tissue-engineered constructs with high cell viability. Biomaterials 2014; 35: 49-62.
27. Yin J, Yan M, Wang Y, Fu J, Suo H. 3D Bioprinting of Low-Concentration Cell-Laden Gelatin Methacrylate (GelMA) Bioinks with a Two-Step Cross-linking Strategy. ACS Appl Mater Interfaces 2018; 10: 6849-6857.